STUDY OF NAMBU AND CHO-MAISON MONOPOLE - ANTIMONOPOLE PAIR IN WEINBERG - SALAM MODEL

ZHU DAN

UNIVERSITI SAINS MALAYSIA

2024

STUDY OF NAMBU AND CHO-MAISON MONOPOLE - ANTIMONOPOLE PAIR IN WEINBERG - SALAM MODEL

by

ZHU DAN

Thesis submitted in fulfillment of the requirements
for the degree of
Doctor of Philosophy

December 2024

ACKNOWLEDGEMENT

First and foremost, I would like to express my sincere gratitude to my supervisor, Dr. Wong Khai Ming, for his guidance, support, and invaluable advice throughout the course of this research. Without his patience and encouragement, this dissertation would not have been possible.

I am also grateful to School of Physics and Theoretical Lab for providing me with the necessary facilities to carry out this research. The computational resources were essential in obtaining the data required for this study.

I owe a great debt of gratitude to my parents, whose unwavering support and encouragement made it possible for me to study abroad. A special thank you goes to my loving wife, who took care of my parents while I was away. She shared the burden with me without complaint, and I am nothing but grateful for her unconditional support and understanding.

Of course, my labmate, Mr. Wong Guo Quan, deserves special thanks for his helpful advice, insightful conversations, and assistance with programming.

Once again, I would like to express my appreciation to everyone who contributed to this research, in ways both big and small. Thank you all for playing an important role in helping me achieve this accomplishment.

TABLE OF CONTENTS

LIST OF TABLES

Page

LIST OF FIGURES

Page

LIST OF ABBREVIATIONS

BNL	Brookhaven National Laboratory
BPS	Bogomol'nyi-Prasad-Sommerfield
CDF	Collider Detector at Fermilab
CERN	Conseil Européen pour la Recherche Nucléaire
CODATA	Committee on Data of the International Science Council
DESY	Deutsches Elektronen-Synchrotron
GG	Georgi-Glashow
GUT	Grand Unified Theory
LBL	Lawrence Berkeley National Laboratory
LHC	Large Hadron Collider
MAC	Monopole-Antimonopole Chain
MAP	Monopole-Antimonopole Pair
PS	Pati-Salam
QCD	Quantum Chromodynamics
QED	Quantum Electrodynamics
QFT	Quantum Field Theory
SK	Super-Kamioka Neutrino Detection Experiment
SLAC	Stanford Linear Accelerator Center
SUGRA	Supergravity
SUSY	Supersymmetry
ToE	Theory of Everything
UA1, UA2	Underground Area 1, 2
VEV	Vacuum Expectation Value
WS	Weinberg-Salam
YMH	Yang-Mills-Higgs

LIST OF SYMBOLS

Z^0	Neutral intermediate vector boson
m_{Z}	Mass of Z^0
$\mathrm{W}^{\pm}$	Charged intermediate vector boson
m_{W}	Mass of $\mathrm{W}^{\pm}$
m_{H}	Mass of the Higgs boson
m_{e}	Mass of the electron
e^{em}	Unit electric charge
a_{e}	Anomalous magnetic moment of electron
α_{F}	Fine structure constant
m	Mass of the field quanta
ψ	A spinor field
$\overline{\psi}$	Adjoint spinor of ψ
γ_μ, γ_0	Gamma matrices
$\phi\left(x, y, z, t\right)$	A scalar field
Ψ	Wave function
$\lvert\Psi\rvert$	Amplitude of Ψ
ϕ_Ψ	Phase of Ψ
$\boldsymbol{v}$	Charged particle velocity
$\boldsymbol{p}$	Momentum vector
$\boldsymbol{r}$	Position vector
r	Radial coordinate (spherical)
ρ	Radial coordinate (cylindrical)
x	Dimensionless radial coordinate
x_c	Compactified radial coordinate
V	Volume
dV	Volume element

S, S_+, S_-	Surfaces
D^2_{xy}, H^2_+	
$d\boldsymbol{S}, dS^i$	Surface element
l	Line path
$d\boldsymbol{l}$	Line element
L	Lagrangian
$\mathcal{L}$	Lagrangian density
$\mathcal{T}$	Kinetic part of $\mathcal{L}$
$\mathcal{V}$	Potential part of $\mathcal{L}$
$q_{\mathrm{e}}, q_{\mathrm{t}}$	Electric charge
ρ_{E}	Electric charge density
$\boldsymbol{J}_{\mathrm{E}}$	Electric current density
q_{m}	Magnetic charge
$q_{\mathrm{m}(S_+)}$	Magnetic charge enclosed in the upper hemisphere (S_+)
$q_{\mathrm{m}(S_-)}$	Magnetic charge enclosed in the lower hemisphere (S_-)
$\rho_{\mathrm{m}}, \mathcal{M}$	Magnetic charge density
$\boldsymbol{J}_{\mathrm{m}}$	Magnetic current density
$\delta^3(\boldsymbol{r})$	Dirac delta function
ε_0	Vacuum permittivity
Φ_{e}	Electric flux
Φ_{m}	Magnetic flux
i, j	Spatial index
μ, ν	Minkowski spacetime index
a, b, c	SU(2) gruop internal index
$F_{\mu\nu}$	SU(2) field strength tensor
$F^a_{\mu\nu}$	SU(2) field strength tensor (adjoint representation)
A_μ	SU(2) gauge field
A^a_μ	SU(2) gauge field (adjoint representation)

g	SU(2) gauge coupling constant
$f_{\mu\nu}$	U(1) field strength tensor
B_μ	U(1) gauge field
g'	U(1) gauge coupling constant
Φ^a	Higgs field (adjoint representation)
μ_{H}	Higgs field mass
ξ, H_0	Higgs field VEV
α	Higgs field inclination angle
$\hat{\mathbf{\Phi}}$	Higgs field unit vector
$H, \lvert\Phi\rvert$	Higgs modulus
$\lvert\Phi\rvert_\infty$	Higgs modulus at spatial infinity
$\lvert\Phi\rvert_O$	Higgs modulus at the origin
λ, β	Higgs self-coupling
β_c	Upper bound in β
θ_{W}	Weinberg angle
$\boldsymbol{\phi}$	Complex scalar Higgs doublet
ϕ^+	Charged component of the Higgs field
ϕ^0	Neutral component of the Higgs field
V_{e}	Electric scalar potential
$\boldsymbol{E}, E_i$	Electric field
$\boldsymbol{A}$	Magnetic vector potential
$\boldsymbol{B}, B_i, B_i^{\text{em}}$	Magnetic field
ε_{abc}	Levi-Civita symbol
$\delta_{\mu\nu}, \delta_b^a$	Kronecker delta
E	Total energy
$\bar{E}$	Mean value of E
E_{min}	BPS bound
$T_{\mu\nu}$	Energy-momentum tensor

ε	Energy density
$\varepsilon_{\text{U(1)}}$	Energy density contribution from the U(1) gauge field
$\varepsilon_{\text{SU(2)}}$	Energy density contribution from the SU(2) gauge field
ε_{H}	Energy density contribution from the Higgs field
ε_{W}	Combined weighted energy density
$g_{\mu\nu}$	Metric tensor
$\lvert g_{\mu\nu}\rvert$	Determinant of $g_{\mu\nu}$
E_i^a	SU(2) Electric field (adjoint representation)
B_i^a	SU(2) Magnetic field (adjoint representation)
ψ_1	Profile function for the SU(2) gauge field
ψ_2	Profile function for the SU(2) gauge field
R_1	Profile function for the SU(2) gauge field
R_2	Profile function for the SU(2) gauge field
τ_1	Profile function for the SU(2) gauge field (temporal)
τ_2	Profile function for the SU(2) gauge field (temporal)
B_1	Profile function for the U(1) gauge field
B_s	Profile function for the U(1) gauge field
B_0	Profile function for the U(1) gauge field (temporal)
Φ_1	Profile function for the Higgs field
Φ_2	Profile function for the Higgs field
$\hat{\boldsymbol{r}}_i$	Ordinary radial unit vector
$\hat{\boldsymbol{\theta}}_i$	Ordinary polar unit vector
$\hat{\boldsymbol{\phi}}_i$	Ordinary azimuthal unit vector
n	ϕ-winding number
$\hat{\boldsymbol{n}}_r^a, \hat{\boldsymbol{r}}^a$	Isospin radial unit vector
$\hat{\boldsymbol{n}}_\theta^a, \hat{\boldsymbol{\theta}}^a$	Isospin polar unit vector
$\hat{\boldsymbol{n}}_\phi^a, \hat{\boldsymbol{\phi}}^a$	Isospin azimuthal unit vector
$\hat{\boldsymbol{u}}_r^a$	Unit vector similar to $\hat{\boldsymbol{n}}_r^a$ used while applying the unitary gauge

$\hat{\boldsymbol{u}}_\theta^a$	Unit vector similar to $\hat{\boldsymbol{n}}_\theta^a$ used while applying the unitary gauge
$\hat{\boldsymbol{u}}_\phi^a$	Unit vector similar to $\hat{\boldsymbol{n}}_\phi^a$ used while applying the unitary gauge
K, J, H	Profile functions for Julia-Zee dyon
D_μ	Covariant derivative
$\mathcal{D}_\mu$	Covariant derivative of the SU(2)×U(1) gauge group
σ_a	Pauli matrices
μ_m	Magnetic dipole moment
d_z	Pole separation
$B_i^{\mathrm{U(1)}}$	U(1) magnetic field
$B_i^{\mathrm{SU(2)}}$	SU(2) magnetic field
A_μ^{em}	Electromagnetic field
Z_μ	Neutral field
R_+	The upper region defined in the Wu-Yang formalism
R_-	The lower region defined in the Wu-Yang formalism
$\boldsymbol{A}_+$	Magnetic vector potential of a Dirac monopole in R_+
$\boldsymbol{A}_-$	Magnetic vector potential of a Dirac monopole in R_-
I_n	Identity matrix of order n
G	A gauge transformation
†	Hermitian transpose
σ_s	Sample standard deviation
c	Speed of light
$\hbar$	Reduced Planck constant
M, N	Grid size
(p, q)	A point on the grid
$[a, b]$	Commutator of a and b
$\{a, b\}$	Anticommutator of a and b
$\boldsymbol{F}_{\mathrm{L}}$	Lorentz force
D	Difference in symmetry

RD	Relative difference in $\lvert\Phi\rvert$
$\epsilon\left(\phi\right)$	U(1) hypercharge permeability
$\mathcal{O}\left(x\right)$	Big O notation
$\pi_n\left(X\right)$	Homotopy gruops of space X

LIST OF APPENDICES

KAJIAN TENTANG PASANGAN MONOKUTUB - ANTIMONOKUTUB NAMBU DAN CHO-MAISON DALAM MODEL WEINBERG - SALAM

ABSTRAK

Dalam disertasi ini, dua jenis penyelesaian pasangan monokutub-antimonokutub (MAP) ditemui dalam modal Weinberg-Salam. MAP adalah sangat penting. Ini kerana jika monokutub magnet dikesan dalam makmal, ia akan melalui pengeluaran pasangan, iaitu konfigurasi yang diterangkan oleh MAP. Dalam kerja ini, MAP Nambu telah disiasat terlebih dahulu, yang terdiri daripada monokutub dan antimonokutub yang dibatasi oleh rentetan fluks Z^0. Ia juga disahkan bahawa MAP Nambu ialah sphaleron elektrolemah, yang memainkan peranan penting dalam baryogenesis. Dalam penyelidikan ini, 300 penyelesaian berangka diperoleh sepadan dengan MAP Nambu dengan gandingan diri Higgs fizikal, $\beta = 0.7782$, dan sudut Weinberg, $\tan\theta_{\rm w} = 0.5358$. Jumlah tenaga penyelesaian ini dikira dan disahkan bahawa ia berada dalam julat 13.17–21.02 TeV. Jisim selebihnya sistem dianggarkan 14.17 ± 0.49 TeV yang sangat menunjukkan bahawa konfigurasi ini mungkin dikesan dalam masa terdekat. Di samping itu, bukti ditemui menunjukkan fenomena berayun dalam ketumpatan tenaga di sepanjang rentetan yang menghubungkan kutub, dikaitkan dengan simetri penyelesaian. Siasatan lanjut mendedahkan bahawa kedua-dua ketumpatan caj magnet dan arus elektrik medan tolok U(1) mempamerkan corak yang sama, yang menyumbang secara langsung kepada ayunan ketumpatan tenaga. Akhirnya, caj magnet penyelesaian ini dikira secara berangka dan telah disahkan bahawa nilainya sememangnya $\pm 4\pi \sin^2\theta_{\rm w}/e^{\rm em}$ seperti yang diramalkan, dengan eem ialah caj elektrik unit. MAP jenis kedua yang dikaji dalam karya ini ialah sepasang monokutub Cho-Maison dan antimonokutub. Pada masa ini, hanya satu- dan n- konfigurasi monokutub telah dikaji untuk jenis monokutub ini dan di sini, kami membentangkan penyelesaian Cho-Maison MAP simetri paksi yang pertama. Sistem ini mula-mula dikaji dengan menetapkan $\tan\theta_{\rm w} = 0.5356$, sambil membenarkan gandingan diri Higgs berubah-ubah ($0 \leq \beta \leq 1.7704$). Dan kemudian, β ditetapkan pada 0.7782, manakala $\tan\theta_{\rm w}$ berjalan dari 0.4675 hingga 10. Momen dipol

magnetik, μ_m, dan pemisahan kutub, d_z, daripada penyelesaian dikira dan dianalisis. Khususnya, apabila kedua-dua parameter adalah fizikal, μ_m MAP Cho-Maison ialah 8.55 dalam unit $1/\left(e^{\text{em}} \cdot m_{\text{W}}\right)$, dengan m_{W} ialah jisim $\text{W}^{\pm}$ boson, dan d_z ialah 8.20 dalam unit $1/m_{\text{W}}$. Akhir sekali, jumlah tenaga bagi konfigurasi ini adalah tidak terhingga disebabkan oleh singulariti titik di lokasi monokutub dan analisis singulariti menyeluruh telah dilakukan.

STUDY OF NAMBU AND CHO-MAISON

MONOPOLE - ANTIMONOPOLE PAIR IN WEINBERG - SALAM MODEL

ABSTRACT

In this dissertation, two types of monopole-antimonopole pair (MAP) solutions are found in the Weinberg-Salam model. The MAPs are of crucial importance. This is because if magnetic monopoles were detected in the lab, it would be through pair production, which is precisely the configuration described by the MAPs. In this work, Nambu MAP was investigated first, which consists of a monopole and an antimonopole bounded by a Z^0 flux string. It was also confirmed that the Nambu MAP is the electroweak sphaleron, which plays an important role in baryogenesis. In this research, 300 numerical solutions were obtained corresponding to the Nambu MAP with physical Higgs self-coupling, $\beta = 0.7782$, and Weinberg angle, $\tan\theta_{\rm w} = 0.5358$. Total energies of these solutions were calculated and confirmed that they reside in a range of 13.17–21.02 TeV. The rest mass of the system was estimated to be 14.17 ± 0.49 TeV which strongly indicates that this configuration might be detected in the near future. In addition, evidence was found indicating an oscillatory phenomenon in the energy density along the string connecting the poles, associated with the symmetry of the solutions. Further investigations revealed that both magnetic charge density and electric current of the U(1) gauge field exhibit similar patterns, which contribute directly to the energy density oscillation. Finally, magnetic charges of these solutions were calculated numerically and it has been confirmed that their values are indeed $\pm 4\pi \sin^2\theta_{\rm w}/e^{\rm em}$ as predicted, with $e^{\rm em}$ being the unit electric charge. The second type of MAPs studied in this work is a pair of Cho-Maison monopole and antimonopole. Currently, only one- and n-monopole configurations have been studied for this type of monopoles and here, we present the first ever axially symmetrical Cho-Maison MAP solutions. The system was first studied by fixing $\tan\theta_{\rm w} = 0.5356$, while allowing the Higgs self-coupling to vary ($0 \leq \beta \leq 1.7704$). And then, β was fixed at 0.7782, while $\tan\theta_{\rm w}$ runs from 0.4675 to 10. Magnetic dipole moment, μ_m, and pole separation, d_z, of the solutions

are calculated and analyzed. In particular, when both parameters are physical, μ_m of the Cho-Maison MAP is 8.55 in unit of $1/\left(e^{\text{em}} \cdot m_{\text{w}}\right)$, where m_{w} is the mass of $\text{W}^{\pm}$ boson, and d_z is 8.20 in unit of $1/m_{\text{w}}$. Lastly, total energy of this configuration is infinite due to point singularities at the locations of monopoles and a thorough singularity analysis was performed.

CHAPTER 1

INTRODUCTION

1.1 Modern Physics before the 1970s

1.1.1 The Cornerstones

The 20th century is a golden age for modern physics. In 1905, a year that earned the *Annus Mirabilis* (Latin for "Marvelous Year") status in Western history, the then 26-year-old Albert Einstein published the four papers that revolutionized our understandings of the fundamental concepts of space, time, mass, and energy. In the third paper he published that year, "Zur Elektrodynamik bewegter Körper" (Einstein, 1905) or "On the Electrodynamics of Moving Bodies" in English, he boldly put forward two postulates that later became the basis of special relativity, a household name even children in kindergarten might heard of today. A decade later, once again, the genius mind gifted the world "Die Grundlage der allgemeinen Relativitätstheorie" (Einstein, 1916) or "The Foundation of the General Theory of Relativity" as translated by Alfred Engel (Einstein, 1916/1996). At present time, both theories of relativity are considered one of the two cornerstones of modern physics, with the other one being quantum mechanics.

In 1900, Max Planck proposed a statistical approach to solve a conundrum that the physics community was facing at the time (Planck, 1900). A conundrum that was later referred to as the "ultraviolet catastrophe". By assuming that the electromagnetic radiation can only be emitted or absorbed in discrete packets, Planck was able to obtain a formula that tends to the Rayleigh-Jeans law in the limit of low frequencies, while at the same time, reproduces the Wien approximation at high frequencies. However, even Planck himself described this approach as "an act of desperation" (Hermann, 1972) because, at the time, there was no reason to assume that energy should be radiated in quanta. Nevertheless, the paper he published in 1900 is now viewed as the beginning of quantum mechanics. For this reason, like Abraham Fraenkel wrote in his memoir, Max Planck is considered the father of quantum theory by many (Fraenkel, 2016, p. 96). However, unlike the theories of relativity, which are largely attributed to

one person, quantum mechanics is the wisdom of numerous scientists who had gone through decades of discoveries, such as Erwin Schrödinger, Niels Bohr, Paul Dirac, Enrico Fermi, Max Planck himself, just to name a few.

In the grand scheme of things, near light speed objects and physical systems where gravity cannot be ignored are governed by the theories of relativity, whereas quantum mechanics focuses on the building blocks of our universe, such as atoms, elementary particles, etc. Both theories have seen tremendous success in their respective fields and thus, the next logical step is to unify the two. However, even though special relativity was integrated into quantum mechanics in the late 1940s, resulting in the quantum electrodynamics (QED), the quantization of general relativity is beset with great problems. As Lewis Ryder explained, in order to do so, there are mathematical, conceptual and practical problems that need to be addressed (Ryder, 1996, p. 2). By the time of his writing, gravitational waves were not yet detected. So today, the practical problems he put forward are partially solved. Still, the endeavor to completely merge the two cornerstones of modern physics into a single, all-inclusive theory is still one of the most formidable task of the 21st century.

1.1.2 The Journey and Significance of QED

While quantum gravity is obviously more daunting, the journey of QED is not exactly smooth. The very first attempt was made by Paul Dirac (1927). In a paper published in 1927, he coined the word "quantum electrodynamics". This paper later led to the formulation of a relativistic wave function, the Dirac equation, that is consistent with both quantum mechanics and special relativity (Dirac, 1928). In the following years, many physicists were dedicated to applying the same principle to fields. Finally in 1932, an elegant formulation of QED was brought forth by Enrico Fermi (1932) that seemed able to describe all forms of electromagnetic interactions. However, with improvements in microwave technology, precise measurements revealed physical phenomena that cannot be explained by Dirac equation, like Lamb shift and the anomalous magnetic moment of electron. Worse still, people soon realized that Fermi's QED is

only reliable for first order perturbation theories as integrations for higher order corrections usually diverge to infinity. For nearly two decades, there was no solutions and some even believed that there existed a fundamental incompatibility between special relativity and quantum mechanics. On a side note, the reason Fermi's formulation worked is because the coupling in QED is the fine structure constant, $\alpha_{\mathrm{F}} \approx 1/137$, which is small enough so that higher order corrections contribute significantly smaller and calculations that include only the simplest Feynman diagrams can still be a good approximation. This, however, no longer holds true for weak and strong interactions.

A silver lining occurred in 1947, a paper of only three pages long and containing merely twelve equations was written by Hans Bethe (1947). He realized that by replacing the theoretically postulated quantities with their experimentally observed values, the term representing self-interactions in the integrand would increase logarithmically instead of linearly, making the integral finite. This method is now known as renormalization. In the years that follow, based on his work and with the efforts of several physicists, particularly Richard Feynman, Julian Schwinger and Shinichiro Tomonaga, QED became a coherent theory that is covariant and gauge invariant. Eventually in 1949, Freeman Dyson definitively proved that QED is renormalizable for any order perturbation theories (Dyson, 1949).

Being one of the most successful branches of physics, QED accurately predicted the anomalous magnetic moment of electron, a_{e}, to an astonishing precision. Theoretically, accounting for 6354 tenth order Feynman diagrams (without closed lepton loops), the value of a_{e} has been calculated to the order of α_{F}^5 (Aoyama et al., 2015):

$$a_{\mathrm{e}} = 0.001\ 159\ 652\ 181\ 643\,(763)\,. \tag{1.1}$$

And the experimentally measured value is (Hanneke et al., 2011):

$$a_{\mathrm{e}} = 0.001\ 159\ 652\ 180\ 73\,(28)\,. \tag{1.2}$$

They agree to nine significant figures, a major triumph that will definitely go down in

history. Today, QED has already become the model and template for all subsequent quantum field theories (QFT) because of its increasing success and, more importantly, a mathematical feature that can be generalized, called gauge invariance.

1.1.3 Gauge Theories, Higgs Mechanism and Renormalizability

To every differentiable symmetry generated by local actions, there is a corresponding conserved current. This is known as Noether's first theorem (Noether, 1918/2006). Indeed, modern physics is built around symmetry and for all QFTs, it is manifested through gauge invariance, a kind of internal symmetry that is independent of the spacetime coordinates. Specifically, in the case of QED, when a phase factor, $e^{i\theta(x)}$, is applied to a spinor field, ψ, that is, $\psi \to e^{i\theta(x)}\psi$, the Lagrangian density, $\mathcal{L}$, remains unchanged. We say that $\mathcal{L}$ exhibits a gauge symmetry and the particular choice of $e^{i\theta(x)}$ is called a gauge.

The concept of gauge theories is not exclusive to modern physics, Maxwell's electromagnetism is an example of classical gauge theories. The electric field, $\boldsymbol{E} = -\nabla V_{\mathrm{e}} - \partial \boldsymbol{A}/\partial t$, and magnetic field, $\boldsymbol{B} = \nabla \times \boldsymbol{A}$, remain unchanged if the following changes are made to the corresponding potentials:

$$V_{\mathrm{e}} \to V_{\mathrm{e}} - \frac{\partial f}{\partial t}, \quad \boldsymbol{A} \to \boldsymbol{A} + \nabla f, \tag{1.3}$$

for any scalar field f. However, the invariance of $\boldsymbol{E}$ and $\boldsymbol{B}$ under transformation (1.3) was not immediately established as a type of symmetry when the theory was first formulated in the late 19$^{\text{th}}$ century. It is just like physicists did not realize the underlying mathematical structure of gauge theories is groups (a concept mathematicians are already familiar with at the time) until Chen-Ning Yang and Robert Mills generalized the idea to non-abelian gauge theories (Yang & Mills, 1954), even though the concept already existed in the 1940s. So now, in terms of group theory terminologies, QED exhibits a U(1) gauge symmetry and is invariant under gauge transformations of the form $e^{i\theta(x)} \in \mathbb{C}$. Obviously, the U(1) gauge group is abelian as complex numbers commute under multiplication. Yang-Mills theory, on the other hand, is more generalized and

based on the SU(N) gauge group or special unitary group of degree N. Because in general, $AB \neq BA$ for two unitary matrices and therefore, it is non-abelian.

The initial goal of Yang-Mills theory was to provide an explanation to the strong interactions between protons and neutrons (by the time, the quark model was not yet proposed). However, as Wolfgang Pauli pointed out, the gauge bosons of Yang-Mills theory are massless, which indicates that the corresponding interactions must have a long range. Like in QED, the massless photons mediate the long-distance electromagnetic interactions. This, however, contradicts the fact that strong interactions are only observed in extremely short distances, around 10^{-15}m. For this reason, Yang-Mills theory was put on hold until the concept of spontaneous symmetry breaking was put forward. Eventually in 1964, three independent groups published papers on a process now known as the Higgs mechanism (Higgs, 1964; Englert & Brout, 1964; Guralnik, Hagen, & Kibble, 1964), the massless problem was solved. Simply put, by adding an all-permeating quantum field (the Higgs field), the gauge symmetries are spontaneously broken below a critical temperature. The broken symmetry then triggers the Higgs mechanism, causing the bosons it interacts with to acquire mass.

Sadly, that was not the only obstacle non-abelian gauge theories were facing. At first glance, it seemed like they were also non-renormalizable and the exact method used for QED does not apply to them. The situation was dire, so much so that if they cannot be renormalized, the whole idea of describing physical interactions using gauge theories is scientifically meaningless. Moreover, unlike Fermi's QED, a similar theory for other interactions is not even possible, because the coupling constant for strong forces, for example, is roughly of the order of one, which means higher order Feynman diagrams contribute just as much as simple ones. Fortunately, as it turned out, only a different renormalization scheme was needed in order to remove the infinities in these theories and the mathematical proof that spontaneously broken gauge symmetries are renormalizable for any order perturbation theories was given by Gerard 't Hooft ('t Hooft, 1971), just like what Freeman Dyson did for QED in 1949.

1.1.4 The Proliferation of QFT

At this point, it is fairly clear now that gauge invariance, Higgs mechanism, and renormalizability are the three legs of the milking stool that is QFT and these three criteria later became the blueprint for manufacturing more sophisticated tools for physicists. Under this new paradigm, a multitude of revolutionary theories emerged. The electromagnetic and weak interactions were unified in the SU(2)×U(1) Weinberg-Salam (WS) theory. The strong interaction between quarks was described in quantum chromodynamics (QCD) which exhibits an SU(3) gauge symmetry. Now, everything except gravity is incorporated in the so-called Standard Model, an SU(3)×SU(2)×U(1) QFT.

The above sums up the journey of modern theoretical physics from the early 20^{th} century to the 1970s, when the Standard Model began to take shape. In the next section, we are going to take a look at the achievements and flaws of this physics masterpiece.

1.2 The Standard Model in a Nutshell

1.2.1 Achievements

Being mathematically elegant alone is not enough for a physics theory, the experimental verification of its predictions matters even more. In the mid 1970s, when the phrase "Standard Model" just started to appear, only three types of quark (up, down, and strange) and four types of lepton (electron, muon, and their corresponding neutrinos) were observed experimentally and none of the gauge bosons, other than photon, was detected.

Chronologically, the first sign of success occurred in 1973 when Conseil Européen pour la Recherche Nucléaire (CERN) confirmed the existence of neutral current (CERNCourier, 2004a). It is a kind of subatomic particle interaction mediated by the neutral Z^0 boson, one of the three intermediate vector bosons responsible for the weak interaction. The discovery of individual $W^{\pm}$ and Z^0 bosons had to wait for the construction of particle accelerators powerful enough to produce them. In 1974, the fourth quark, charm, was detected by two independent groups, one at the Stanford Linear Ac-

celerator Center (SLAC), led by Burton Richter (Augustin et al., 1974) and the other at the Brookhaven National Laboratory (BNL), led by Samuel Ting (Aubert et al., 1974). This marked the complete detection of the first two generations of elementary particles predicted by the Standard Model. Specifically, electron, electron neutrino, up and down quarks belong to the first generation. Muon and its neutrino, along with strange and charm quarks are in the second generation.

Soon after, the lepton tauon was detected in a series of experiments between 1974 and 1977 (Okun, 1980, p. 103) by Martin Lewis Perl et al. (1975) at SLAC and Lawrence Berkeley National Laboratory (LBL). Its accompanying neutrino, however, was detected much later in history. Then, the bottom quark was found in 1977 at Fermilab by a group led by Leon M. Lederman (Fermilab, 1977). The existence of gluons, the gauge bosons of strong interaction, was confirmed in 1979 at Deutsches Elektronen-Synchrotron (DESY) by the PLUTO Collaboration (1979), where the characteristic three-jet event was observed. On a side note, because of the nature of the SU(3) gauge symmetry of QCD, there are eight distinct kinds of gluon. However, it is not possible to isolate them due to color confinement. Though, there are some interesting news regarding deconfinement and quark-gluon plasma, individual gluons are not detected to this day. On the other hand, each and every gauge boson for the weak interaction was produced in 1983 at CERN through the Underground Area 1 (UA1) and UA2 experiments (CERNCourier, 2004b).

Then came a decade of silence for experimental particle physics, mostly because the precision and energy threshold of the then top-of-the-line facilities were not high enough to produce the remaining elementary particles predicted by the Standard Model. In 1995, top quark was detected by both the Collider Detector at Fermilab (CDF) and the D0 experiment (CDF Collaboration, 1995; D0 Collaboration, 1995). Six years later, the Direct Observation of the Nu Tau (DONUT) at Fermilab announced the discovery of tauon neutrino (DONUT Collaboration, 2001), which completed the confirmation of the existence of all three generations of quarks and leptons predicted by the Standard Model. Finally, the last piece of the puzzle, Higgs boson—the “God par-

ticle" that bestows mass—was found in 2012 at the Large Hadron Collider (LHC) after countless of experiments conducted in the course of three years and with two groups of experimenters working independently (Overbye, 2013).

Today, the Standard Model is indubitably the most successful collection of theories in modern physics. All constituents predicted have been found experimentally, which include 12 types of "building block" (three generations of quarks and leptons), four types of force carriers (photon, $W^{\pm}$, Z^0 bosons, and gluon) and the only scalar boson—the Higgs particle. The tremendous success of the past 50 years clearly indicated that the Standard Model is indeed the correct representation of the universe. However, no one in the field of physics would claim that it is the final picture as there are numerous questions left unexplained and unanswered.

1.2.2 Shortcomings

There are four fundamental forces exist in nature, namely weak, strong, electromagnetic forces, and gravity. The most glaring inadequacy of the Standard Model is that only three of them are accounted for. On 14 September 2015, first direct observation of gravitational waves was made through a joint effort by Laser Interferometer Gravitational-Wave Observatory (LIGO) and the Virgo Collaboration, the announcement was made a year later (LIGO Scientific Collaboration and Virgo Collaboration, 2016). Such a discovery, once again, demonstrated the validity of Einstein's general relativity, which made the incorporation of gravity into the current theoretical framework even more urgent.

Secondly, there is the missing baryon problem or baryon asymmetry. Even though all antimatter particles predicted by the Standard Model have been found, the observable universe consists almost exclusively of matter, where did all the antimatter go when the Big Bang was supposed to create an equal amount of matter and antimatter to maintain charge neutrality? Neither the Standard Model, nor the general theory of relativity provides an explanation to this established fact. Presumably, some laws might function differently for matter or antimatter that physicists are not aware of. For this

reason, the baryon asymmetry is described as "one of the great mysteries in physics" (Canetti, Drewes, & Shaposhnikov, 2012). Additionally, the hypothesized physical process responsible for the baryon asymmetry is called baryogenesis.

According to the data gathered by the Planck spacecraft, the universe contains only 4.82% $\pm$ 0.05% of ordinary matter, the rest comes from dark matter (25.8% $\pm$ 0.4%) and dark energy (69% $\pm$ 1%) (Planck Collaboration, 2013) for which the Standard Model offers no explanation. Ironically, the collection of extremely complicated theories physicists spent nearly a century to perfect can only be used to give a semi-satisfactory description for roughly 5% of the universe. Moreover, the Standard Model itself is not mathematically elegant from an aesthetics point of view. Some physicists consider it to be ad hoc as there are roughly 20 unrelated, arbitrary constants (Cahn, 1996), like the mass of every elementary particle, the gauge coupling constants, etc., whose values can only be determined through experimental measurements and theoretical explanations on these constants are completely inadequate.

On top of that, recent development in experimental physics shows signs of discrepancy between experimental measurements and theoretical predictions, suggesting physics beyond the Standard Model maybe having an effect. In 2017, measurements of the anomalous magnetic moment of muon disagreed with the Standard Model by 3.5 standard deviations (Giusti, Lubicz, Martinelli, Sanfilippo, & Simula, 2017). In April 2022, the CDF Collaboration reported the latest measurements of the mass of $\mathrm{W}^{\pm}$ boson, $m_{\mathrm{W}} = 80,433 \pm 9$ MeV (CDF Collaboration, 2022), which is seven standard deviations above the predicted value.

Therefore, the Standard Model is definitely not the end of modern physics and all of these shortcomings together hint at the possibility of even more all-inclusive theories. A few attempts have already been made in the past several decades, some of them will be briefly discussed in the next section.

1.3 Beyond the Standard Model

1.3.1 Grand Unified Theories

As stated earlier, the electromagnetic and weak forces were united into a single electroweak interaction. Below the unification energy, 246 GeV which is the vacuum expectation value (VEV) of the Higgs field, the SU(2)×U(1)$_Y$ gauge group spontaneously breaks into a U(1)$_{\text{em}}$ gauge symmetry. Note here, the subscript "Y" and "em" represent weak hypercharge and electromagnetism respectively. They are two different instances of the generic U(1) gauge symmetry. Physicists have been trying to apply the same principle to the strong interaction, unifying all three forces into one. Such theoretical frameworks have come to be known as the grand unified theories (GUTs).

Unlike the electroweak interaction, which has a low unification energy that can be produced in the lab, most GUTs require an energy scale of around 10^{16} GeV for the unification to occur. Therefore, any new particle predicted by these GUTs is well above the capability of literally any particle accelerator on Earth. To put things into perspective, the maximum energy that can be produced in the LHC is only 14 TeV, 10^{16} GeV is astronomical. There are numerous competing GUTs today, none of which is universally accepted because they cannot be experimentally verified. Also, it is important to know that in the Standard Model, the electroweak WS theory and QCD representing the strong interaction are referred to as two different sectors, with no unification.

Naturally, GUTs should belong to some higher order gauge symmetries that contain the SU(3)×SU(2)×U(1) gauge group (i.e., the Standard Model) after spontaneous symmetry breaking. Historically, the first true GUT was based on SU(5), proposed by Howard Georgi and Sheldon Glashow (Georgi & Glashow, 1974). Their GUT is also known as the Georgi-Glashow (GG) model. In the same year, Abdus Salam and Jogesh Pati (Pati & Salam, 1974) proposed a model based on the SU(4)×SU(2)×SU(2) gauge group. The most prominent feature of the Pati-Salam (PS) model is that the leptons are viewed as the fourth quark color charge. Both the GG and PS models can be embedded within an SO(10) unification model (Fritzsch & Minkowski, 1975) that is based on the

spin group Spin(10) and the list of GUTs does not stop here.

In the Standard Model, a proton is stable because it is the lightest baryon. In most GUTs, however, the conservation of baryon number can be violated, allowing protons to decay, albeit with extremely long half-life. The predictions of the half-life and mode of proton decay are slightly different among GUTs. For instance, a proton decays into a positron and a pion in the SU(5) GG model, and the half-life is predicted to be around 10^{30}–10^{31} years, whereas in a supersymmetric SU(5) model, it decays into an antineutrino and a kaon, and the half-life is 10^{28}–10^{32} years (Bueno et al., 2007) (more on supersymmetry in the next subsection). In general, the range is between 10^{28} and 10^{36} years, which is insanely long, considering the age of the universe is only 10^{10} years (Griffiths, 2008, p. 33). However, given the gargantuan amount of atoms in the universe, it is not impossible to detect proton decay experimentally. The Super-Kamioka Neutrino Detection Experiment (SK) located in Japan is designed to detect proton decays, among other purposes. It uses 50,000 metric tons of ultrapure water to screen for Cherenkov radiation. In 1998, a research team conducted a 414-days-long experiment at SK. Though, not a single sign of proton decay was found, they managed to set a lower limit on the half-life, which is 1.6×10^{33} years with 90% confidence level (Super-Kamiokande Collaboration, 1998). This result vetoed multiple GUTs, like the SU(5) GG model, whose prediction of the half-life for proton decay is shorter.

GUTs are essentially enlarged versions of the Standard Model, so they share both its merits and defects. In most GUTs, gravity is still not incorporated, dark matter and dark energy are still not addressed. Eventually, physicists come up with an idea to theoretically solve all of these problems—supersymmetry (SUSY).

1.3.2 Supersymmetry

Modern theoretical physicists have always been working with internal symmetries that closely link related subatomic particles or quantum numbers, like the flavor symmetry that links all six types of quark, the SU(2) gauge group for isospin (a quantum number pertaining to the up and down quarks), etc. Physical systems are invariant

under rotations within the corresponding space, flavor space, isospin space, etc.

In the 1960s, Japanese physicist Hironari Miyazawa put forward an idea that could be considered as the prototype of SUSY (Miyazawa, 1966, 1968), where both baryons and mesons are grouped together in a supermultiplet. That is, baryons and mesons are viewed as two different manifestations of the same particle state relating through a rotation in a symmetry group. However, the kind of symmetry described in his theory, if there is any, is extremely broken. That is why his work was largely ignored at the time. Years later, his original idea was generalized to a symmetry relating all particles whose spins differ by 1/2 (Wess & Zumino, 1974). Invariance of this kind, linking fermions and bosons, is called SUSY (Griffiths, 2008, p. 412).

Under this theoretical framework, each fermion is assigned a partner boson and vice versa. Collectively, they are known as superpartners or sparticles. For instance, the superpartner of a top quark is called a stop squark, which is a boson with spin-0. While the top quark is the heaviest known quark, the stop squark is often the lightest squark in many SUSY models. In contrast, superpartners of bosons have an -ino appended to their names, like for gluons, there's gluinos (spin-1/2), and for gravitons, gravitinos (spin-3/2). However, all of these seem like a sleight of hand. They are, if not for their deeper theoretical implications.

First off, unlike GUTs or the Standard Model, gravity can be incorporated in SUSY models. The resulting theory is called supergravity (SUGRA). Technically, this is because the generators of SUSY and the Poincaré algebra (related to Minkowski spacetime symmetry) form a superalgebra, called the super-Poincaré algebra. Therefore, SUSY as a gauge theory makes gravity arise naturally (van Nieuwenhuizen, 1981). Theories like this, incorporating all four natural forces, are referred to as Theory of Everything (ToE). Secondly, because SUSY basically doubled the amount of elementary particles, introducing new interactions. The Feynman diagrams representing these interactions must be included in the renormalization process. This alters the energy dependence of the three running coupling constants (electromagnetic, weak, and strong), making their perfect convergence at GUT scale (10^{16} GeV) possible (Griffiths, 2008,

p. 406). A result too marvelous to be taken as a simple coincidence.

Then, there is the so-called hierarchy problem. In the Standard Model, the mass of the Higgs boson is a parameter to be measured, rather than a value to be calculated. However, the actually measured value, 125.10 ± 0.14 GeV (Particle Data Group, 2020), is significantly lowered than expected even if only first-order quantum corrections are considered, giving rise to the hierarchy problem. Obviously, a large amount of fine-tuning is required to "magically" cancel out the effects of these quantum corrections. However, without a satisfactory explanation, this kind of fine-tuning is considered unnatural and the explanation can be provided by SUSY. Because fermionic and bosonic loop corrections are of the opposite sign, by pairing each particle with its sparticle, SUSY makes the cancellation natural and exact. Last but not least, in most SUSY models, the lightest sparticles are colorless, neutral, and stable, making them attractive candidates for dark matter.

Admittedly, SUSY sounds too good to be true. Also, to a lot of physicists' disappointment, there is literally no experimental evidence to suggest any SUSY model might be correct. To quote David Griffiths, "If supersymmetric particles are discovered at the LHC, it will be a spectacular triumph of inspired audacity. But I wouldn't bet your last dollar on it." (Griffiths, 2008, p. 413). However, there is one thing that is required by most GUTs, SUSY models, and might be detected experimentally in the near future—magnetic monopoles, which is also the main topic of this dissertation.

1.4 Magnetic Monopoles

Lodestones are naturally occurring magnets. Early scientists conceived of the naturally magnetized nature of lodestones as coming from two different *effluvia* (in Latin), which is loosely translated to "magnetic fluids" in this context (Chalmers, 1937), a north-pole fluid at one end and a south-pole fluid at the other. It was believed that magnetic monopoles carrying different charges accumulated at opposite sides of a lodestone, forming magnetic fluids and thus, give rise to lodestones' magnetized nature. This could be considered as the earliest account of the concept—magnetic monopole.

Of course, the idea was eventually abandoned because of an improved understanding of electromagnetism in the nineteenth century, which showed that the magnetism of lodestones was the result of a combination of electric currents and magnetic moments of electrons and other particles.

In the mid to late 19th century, James Clerk Maxwell unified magnetism, electricity, light, and their associated radiations through a series of work, reducing the number of equations describing various phenomena from different fields to four—the Maxwell's equations, among which is one called Gauss's law for magnetism:

$$\nabla \cdot \boldsymbol{B} = \oiint_S \boldsymbol{B} \cdot d\boldsymbol{S} = 0, \tag{1.4}$$

shown in both of its differential and integral forms. The zero at the very end of the equation indicates that magnetic monopoles do not exist. However, this assumption is based on the fact that these particles were not observed. It is not because Maxwell's theory intrinsically forbids their existence. In 1894, French physicist Pierre Curie pointed out that magnetic monopoles could conceivably exist (Curie, 1894). However, it is not until almost four decades later did the first complete formalism of a quantum theory of magnetic monopole appear, proposed by Paul Dirac (1931).

The most appealing feature of Dirac monopole is none other than the quantization condition. Simply put, for a system consisting of an electric monopole, q_{e}, and a magnetic monopole, q_{m}, the total angular momentum is proportional to the product, $q_{\mathrm{e}}q_{\mathrm{m}}$. In the context of quantum mechanics, $q_{\mathrm{e}}q_{\mathrm{m}}$ must be quantized and given that the form of Maxwell's equations is intact, this would then force all electric charges in the universe to be quantized. This is known as the Dirac quantization condition. In 1909, the oil drop experiment has already established the fact that electric charges are quantized. However, it is only a necessary condition and therefore, from a logical point of view, it does not guarantee the existence of magnetic monopoles, but a lack of proper explanations as to why they are quantized have led physicists to believe that magnetic monopoles must exist.

From an aesthetics point of view, all of the four Maxwell's equations and the ex-

pression for Lorentz force become completely symmetrical when magnetic monopoles are incorporated. This is tabulated in Table 1.1. Magnetic monopoles introduce magnetic charge, q_{m}, magnetic charge density, ρ_{m}, and magnetic current density, $\boldsymbol{J}_{\mathrm{m}}$. Note that in the last column, both Gauss' laws are identical in forms, the Faraday's law and Ampère's law mirror each other, and the expression for Lorentz force is completely symmetrical. This is yet another piece of theoretical evidence that cannot be taken as a simple coincidence.

Unfortunately, things went quiet for another four decades. No matter how elegant theories might become with Dirac monopoles incorporated, physicists simply could not take the concept seriously because of a major flaw the Dirac monopole has—infinite energy due to a string singularity. In 1969, Tai-Tsun Wu and Chen-Ning Yang found a solution to the Yang-Mills field equations (Wu & Yang, 1969) that was soon identified as a magnetic monopole and therefore, generalizing the idea to the context of gauge theories. However, their solution also has infinite energy for having a potential that behaves like $1/r$ everywhere. Eventually, a significant turn of events happened in 1974, when the first finite energy magnetic monopole solution was found independently by Gerard 't Hooft and Alexander Polyakov ('t Hooft, 1974; Polyakov, 1974) in the SU(2) Yang-Mills-Higgs (YMH) theory, which immediately piqued the interest of the physics community.

Since then, magnetic monopole research flourished, a large amount of work was done in the SU(2) YMH theory, numerous finite energy solutions were found, exact or

Table 1.1: A comparison between forms of certain laws of physics, without or with magnetic monopole, in natural units.

Name	w/o magnetic monopole	w/ magnetic monopole
Gauss's law	$\nabla \cdot \boldsymbol{E} = \rho_{\mathrm{e}}$	
Gauss's law (magnetism)	$\nabla \cdot \boldsymbol{B} = 0$	$\nabla \cdot \boldsymbol{B} = \rho_{\mathrm{m}}$
Faraday's law (induction)	$-\nabla \times \boldsymbol{E} = \partial \boldsymbol{B}/\partial t$	$-\nabla \times \boldsymbol{E} = \partial \boldsymbol{B}/\partial t + \boldsymbol{J}_{\mathrm{m}}$
Ampère's law	$\nabla \times \boldsymbol{B} = \partial \boldsymbol{E}/\partial t + \boldsymbol{J}_{\mathrm{e}}$	
Lorentz force $\boldsymbol{F}_{\mathrm{L}}$	$q_{\mathrm{e}}(\boldsymbol{E} + \boldsymbol{v} \times \boldsymbol{B})$	$q_{\mathrm{e}}(\boldsymbol{E} + \boldsymbol{v} \times \boldsymbol{B}) + q_{\mathrm{m}}(\boldsymbol{B} - \boldsymbol{v} \times \boldsymbol{E})$

numerical. Among these works, there is the monopole-antimonopole pair (MAP) solution found by Kleihaus and Kunz (1999). Essentially, it is a pair of 't Hooft-Polyakov monopole and antimonopole lying symmetrically along the z-axis. Their solution is monumental because if magnetic monopoles are found experimentally, say in the LHC, it is through pair production, which is precisely the configuration described by the MAP solutions. However, the SU(2) YMH theory is not physical, MAP solutions found in the SU(2)×U(1) WS theory will possess more physical significance.

Among all the works done in the electroweak framework, there are two particular lines of research that intrigue the author of this dissertation. In 1977, Yoichiro Nambu demonstrated the existence of a pair of magnetic monopole and antimonopole bound by a flux string in the SU(2)×U(1) WS theory (Nambu, 1977) through theoretical derivation. The total energy of the Nambu MAP configuration is finite and the mass of the system (monopole, antimonopole, together with the string) is estimated to be in the TeV range. In 2015, the Nambu MAP was proven numerically by Teh, Ng, and Wong (2015). The other line of research started from the work of Cho and Maison (1997) in which they proposed an electroweak generalization of the Dirac monopole. Even if their solution, known as the Cho-Maison monopole, possesses infinite energy due to a point singularity at the origin, it is possible to regularize the solution. Several schemes have already been reported (Blaschke & Beneš, 2018; Zhang, Zou, & Cho, 2020). The energy of a Cho-Maison monopole is also estimated to be in the TeV range (Kimm, Yoon, & Cho, 2015; Kimm, Yoon, Oh, & Cho, 2016). A more detailed literature review on the works listed above is presented in the next chapter.

Magnetic monopole research has come a long way and now, we are at a stage where these elusive particles might actually be detected experimentally, if their actual mass is at the lower end of the estimated range. Moreover, predictions of the mass of monopoles seem to be rather model-dependent. Hence, experimental confirmation of magnetic monopoles is vital as it could indicate which GUT or SUSY models are on the right track and which ones should be discarded. Finally, to quote string theorist Joseph Polchinsk (2004), "The existence of magnetic monopoles seems like one of the

safest bets that one can make about physics not yet seen." (p. 152). Today, magnetic monopole remains the most long-awaited particle in the wake of the discovery of Higgs bosons and here, the future of modern physics quietly beckons.

1.5 Research Gap and Objectives

This dissertation focuses on the two lines of research outlined in the previous section. Because of the complexity of axially symmetrical magnetic monopole configurations in the electroweak framework, the amount of work done on MAPs in the SU(2)×U(1) WS model has been scarce. For the Nambu MAP, while Teh et al. (2015) successfully constructed this configuration, the Weinberg angle is chosen to be $\pi/4$ in their calculation. The advantage of this particular choice is that the mathematical derivation and modelling were greatly simplified as it removes a running parameter, the Weinberg angle, from the numerical model altogether. Subsequently, the convergence of solutions can be more readily achieved. Nevertheless, $\pi/4$ is an unphysical value and as a result, the dimension of quantities investigated cannot be addressed. For the second line of research, substantial progress has already been made on the Cho-Maison monopole, which include regularization, mass estimation, topological stability studies, primordial black hole solutions, etc. However, existing studies predominantly focus on the one- or n-monopole configurations.

Thus, we extend these two lines of research in this work. First off, the Nambu MAP solutions constructed by Teh et al. (2015) will be further studied. More specifically, the following objectives are to be achieved:

1. To adopt the physical Weinberg angle and Higgs self-coupling constant to ensure the research possesses physical significance.

2. To properly address the dimensions of all equations of motion and the physical quantities investigated.

3. To estimate the total energy of the Nambu MAP (monopole, antimonopole, together with the string) in units of TeV.

4. To calculate the magnetic charge carried by either the monopole or antimonopole numerically and verify the prediction Nambu made in the 1970s.

Secondly, for the Cho-Maison MAP research, the objectives are as follows:

1. To slightly modify the magnetic ansatz of Nambu MAP and adjust the boundary conditions accordingly, enabling the construction of axially symmetrical Cho-Maison MAP solutions.

2. To verify that the magnetic charges carried by the poles are indeed $\pm 4\pi/e^{\mathrm{em}}$, the characteristic value of a Cho-Maison monopole.

3. To estimate the total energy of the configuration, if possible. Otherwise, to perform a singularity analysis for future regularization purposes.

4. To accurately measure and study the system for physical quantities such as poles separation, magnetic dipole moment, etc.

1.6 Dissertation Outline

This work is divided into eight chapters. A more detailed literature review on monopole research discussed earlier is shown in Chapter 2. The mathematical framework upon which all modern particle physics are built on, gauge theories, is covered in Chapter 3. Theoretical details regarding the construction of Nambu MAPs, physical quantities investigated, numerical method, boundary conditions, etc., are presented in Chapter 4. Results and discussions of Nambu MAP solutions are shown in Chapter 5. There are similar arrangements for the Cho-Maison MAP in Chapter 6 and 7. Finally, some comments and future research suggestions are in the last chapter.

CHAPTER 2

LITERATURE REVIEW ON MAGNETIC MONOPOLES

2.1 From Maxwell's Equations to M-Theory

In the field of theoretical physics, there is a concept called S-duality that relates two seemingly different theories to one another in a non-trivial way. The oldest and classical example is Maxwell's electromagnetism. Now, consider two preexisting electric and magnetic fields, $\boldsymbol{E}$ and $\boldsymbol{B}$, with no external electric charge and current present, the Maxwell's equations look like (in natural units):

$$\begin{aligned} \nabla \cdot \boldsymbol{E} &= 0, \\ \nabla \cdot \boldsymbol{B} &= 0, \\ \nabla \times \boldsymbol{E} &= -\partial \boldsymbol{B}/\partial t, \\ \nabla \times \boldsymbol{B} &= \partial \boldsymbol{E}/\partial t. \end{aligned} \tag{2.1}$$

The above set of equations is invariant under a transformation that simultaneously replaces the electric and magnetic fields:

$$\boldsymbol{E} \to \boldsymbol{B}, \qquad \boldsymbol{B} \to -\boldsymbol{E}. \tag{2.2}$$

Therefore, for a pair of electric and magnetic fields that solve the Maxwell's equations, it is possible to find a different physical setup in which the fields are essentially interchanged, the new setup is still a solution. This is the most basic form of S-duality in field theories. On a side note, S-duality or duality in general is different from gauge invariance discussed earlier, like equation (1.3). Simply put, gauge symmetry is about the field itself, whereas duality is a relationship between two different fields.

Now, back to Maxwell's equations, the electromagnetic duality is broken when an electric charge distribution (with charge density ρ_{e} and current density $\boldsymbol{J}_{\text{e}}$) is intro-

duced into the system:

$$\begin{aligned}
\nabla \cdot \boldsymbol{E} &= \rho_{\mathrm{e}}, \\
\nabla \cdot \boldsymbol{B} &= 0, \\
\nabla \times \boldsymbol{E} &= -\partial \boldsymbol{B}/\partial t, \\
\nabla \times \boldsymbol{B} &= \partial \boldsymbol{E}/\partial t + \boldsymbol{J}_{\mathrm{e}}.
\end{aligned} \tag{2.3}$$

This is the most general form of Maxwell's equations which even undergraduate students in physics are familiar with, but the duality vanishes. However, it can be restored by incorporating magnetic monopoles, which introduce a magnetic charge density ρ_{m} and a current density $\boldsymbol{J}_{\mathrm{m}}$:

$$\begin{aligned}
\nabla \cdot \boldsymbol{E} &= \rho_{\mathrm{e}}, \\
\nabla \cdot \boldsymbol{B} &= \rho_{\mathrm{m}}, \\
\nabla \times \boldsymbol{E} &= -\partial \boldsymbol{B}/\partial t + \boldsymbol{J}_{\mathrm{m}}, \\
\nabla \times \boldsymbol{B} &= \partial \boldsymbol{E}/\partial t + \boldsymbol{J}_{\mathrm{e}},
\end{aligned} \tag{2.4}$$

and now, the set of "revised" Maxwell's equations become invariant under the following transformation:

$$\begin{aligned}
&\boldsymbol{E} \to \boldsymbol{B}, && \boldsymbol{B} \to -\boldsymbol{E}, \\
&\rho_{\mathrm{e}} \to \rho_{\mathrm{m}}, && \rho_{\mathrm{m}} \to -\rho_{\mathrm{e}}, \\
&\boldsymbol{J}_{\mathrm{e}} \to \boldsymbol{J}_{\mathrm{m}}, && \boldsymbol{J}_{\mathrm{m}} \to -\boldsymbol{J}_{\mathrm{e}}.
\end{aligned} \tag{2.5}$$

The above is the implication of Table 1.1 on a deeper level. That is, insisting the existence of magnetic monopoles gives rise to S-duality. Montonen and Olive (1977) were the first to generalize the invariance of the "revised " Maxwell's equations to QFTs, a non-abelian analog to the electromagnetic duality. The motivation is, to quote their own words, "There should be two 'dual equivalent' field formulations of the same the-

ory in which electric (Noether) and magnetic (topological) quantum numbers exchange roles." (Montonen & Olive, 1977, p. 117). Their work is now viewed as the origin of S-duality, which has already become a basic ingredient of modern physics.

More technically, to compute an observable quantity in a QFT, say A, physicists typically apply the methods of perturbation theory by expanding the term:

$$A = A_0 + A_1 g + A_2 g^2 + A_3 g^3 + ..., \tag{2.6}$$

where g is the coupling constant. If $g > 1$, most likely the sum will go to infinity. In this case, the theory is said to be strongly coupled and one cannot use perturbation theory to make predictions. On the other hand, if $g < 1$, higher powers of g become negligibly small and the sum might converge. In this case, the theory is said to be weakly coupled. S-duality links a strongly coupled theory with g to a weakly coupled one with $1/g$, allowing calculations in one theory (where they diverge) to be translated to the other (where calculations are straightforward). For this reason, S-duality is also called strong-weak duality and any two theories related this way are mathematically different descriptions of the same phenomena.

The greatest achievement of S-duality and T-duality (the particulars of this duality are outside of the scope of this dissertation) is unifying five distinct kinds of string theory. The existence of such a theory, now known as M-theory, was first conjectured by Edward Witten (1995), whose announcement kickstarted the so-called second superstring revolution (1995–2003). From Maxwell's equations all the way to M-theory, it all started from magnetic monopoles.

2.2 Dirac Monopole

The fact that certain fundamental physical quantities are discrete or quantized is a revolutionary idea at the turn of the 20$^{\text{th}}$ century. Even the originator of quantum mechanics, Max Planck, was skeptical about atoms and ignored Boltzmann's statistical theory in the late 1890s (Physics World, 2000). The fact that electric charges are quantized was established in 1909 through the oil drop experiment performed by Robert A.

Millikan and Harvey Fletcher. Since then, physicists always regard the quantization of electric charges as one of the axioms of nature. In 1931, Paul Dirac proposed a possible theoretical foundation for this phenomenon (Dirac, 1931) and the protagonist is precisely the Dirac monopole.

In electrostasis, the physics between a source charge, q_{e}, and a test charge, q_{t}, is governed by Coulomb's law (in SI units):

$$\boldsymbol{F} = \frac{1}{4\pi\varepsilon_0}\frac{q_{\mathrm{t}}q_{\mathrm{e}}}{|\boldsymbol{r}_{\mathrm{e}1}|^2}\hat{\boldsymbol{r}}_{\mathrm{e}1} = q_{\mathrm{t}}\boldsymbol{E}, \tag{2.7}$$

where ε_0 is the vacuum permittivity and $\boldsymbol{E}$ is the electric field of q_{e}, which can be expressed as:

$$\boldsymbol{E} = \frac{q_{\mathrm{e}}}{4\pi\varepsilon_0 r^2}\hat{\boldsymbol{r}} = -\frac{q_{\mathrm{e}}}{4\pi\varepsilon_0}\nabla\left(\frac{1}{r}\right), \tag{2.8}$$

the index on the unit vector, $\hat{\boldsymbol{r}}$, is dropped when a test charge is not present. The electric flux, Φ_{e}, through an imaginary sphere, S, enclosing the source charge is:

$$\Phi_{\mathrm{e}} = \oiint_S \boldsymbol{E}\cdot d\boldsymbol{S} = \int_0^{\pi}\int_0^{2\pi}\frac{q_{\mathrm{e}}}{4\pi\varepsilon_0 r^2}\hat{\boldsymbol{r}}\cdot\left(r^2\sin\theta\; d\theta\; d\phi\right)\hat{\boldsymbol{r}} = \frac{q_{\mathrm{e}}}{\varepsilon_0}. \tag{2.9}$$

By the same token, the physics around a magnetic monopole can be similarly constructed. The magnetic field, $\boldsymbol{B}$, of a monopole with magnetic charge, q_{m}, is

$$\boldsymbol{B} = \frac{q_{\mathrm{m}}}{r^2}\hat{\boldsymbol{r}} = -q_{\mathrm{m}}\nabla\left(\frac{1}{r}\right). \tag{2.10}$$

Note that the factor $1/4\pi\varepsilon_0$ is dropped. There might be a magnetic equivalent, but it can be absorbed into q_{m}. The magnetic flux, Φ_{m}, through a Gaussian surface, S, enclosing the monopole is

$$\Phi_{\mathrm{m}} = \oiint_S \boldsymbol{B}\cdot d\boldsymbol{S} = \int_0^{\pi}\int_0^{2\pi}\frac{q_{\mathrm{m}}}{r^2}\hat{\boldsymbol{r}}\cdot\left(r^2\sin\theta\; d\theta\; d\phi\right)\hat{\boldsymbol{r}} = 4\pi q_{\mathrm{m}}. \tag{2.11}$$

In vector calculus, according to Gauss's theorem, there is an equivalence between the flux of a vector field over a closed surface, S, and the volume integral of the

divergence of the field inside S (with volume V):

$$\oiint_S \boldsymbol{B} \cdot d\boldsymbol{S} = \iiint_V \nabla \cdot \boldsymbol{B} dV. \tag{2.12}$$

This will lead to zero magnetic flux because, unlike the electric field, $\boldsymbol{B}$ is defined through a vector potential, $\boldsymbol{A}$:

$$\boldsymbol{B} = \nabla \times \boldsymbol{A}. \tag{2.13}$$

Then, it is obvious that $\boldsymbol{A}$ must not be defined globally. Otherwise, Φ_{m} would vanish as the divergence of a curl is always zero for any smooth vector field. In fact, judging by the form of $\boldsymbol{B}$ shown in equation (2.10), $\boldsymbol{A}$ is indeed singular as the divergence of $\boldsymbol{B}$ is not defined at the origin:

$$\nabla \cdot \boldsymbol{B} = -q_{\text{m}} \nabla^2 \left(\frac{1}{r} \right) = 4\pi q_{\text{m}} \delta^3 (\boldsymbol{r}), \tag{2.14}$$

where $\delta^3 (\boldsymbol{r})$ is the Dirac delta function:

$$\delta^3 (\boldsymbol{r}) = \begin{cases} 0 & \text{if } \boldsymbol{r} \neq 0, \\ \infty & \text{if } \boldsymbol{r} = 0. \end{cases} \tag{2.15}$$

This way, the integral becomes

$$\Phi_{\text{m}} = \iiint_V \nabla \cdot \boldsymbol{B} dV = \iiint_V 4\pi q_{\text{m}} \delta^3 (\boldsymbol{r}) \, dV = 4\pi q_{\text{m}}, \tag{2.16}$$

which is consistent with equation (2.11).

Now, in the context of quantum mechanics, the wave function, Ψ, of a free particle has the following form (in natural units):

$$\Psi = |\Psi| e^{i(\boldsymbol{p} \cdot \boldsymbol{r} - Et)}, \tag{2.17}$$

where $|\Psi|$ is the amplitude, $\boldsymbol{p}$ and $\boldsymbol{r}$ are the momentum and position vectors of the particle, with E being its energy at instant, t. In the presence of the magnetic field

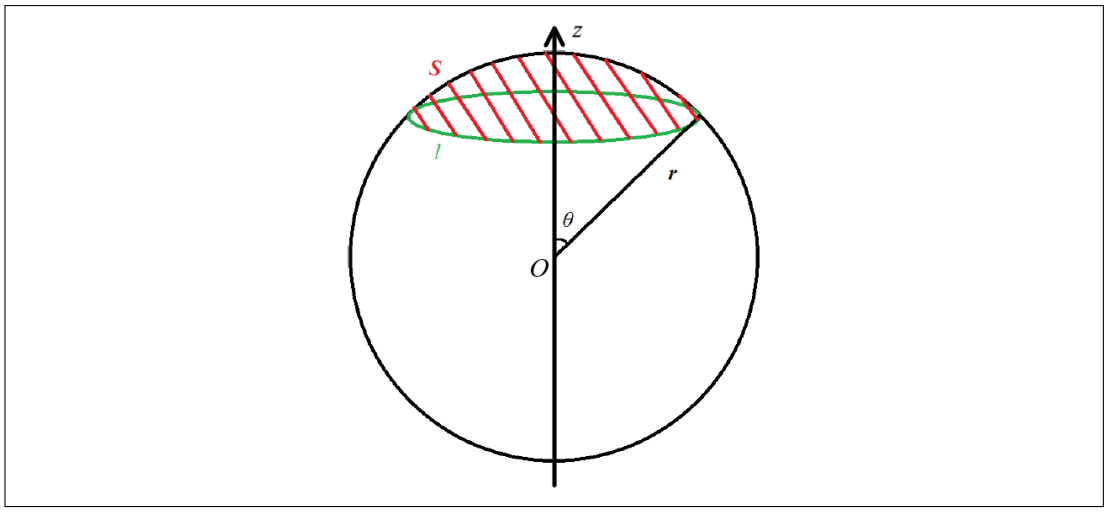

Figure 2.1: A pictorial representation of the closed path l, along with the relationship between the two integrals, shown in equation (2.20).

generated by the monopole, the momentum $\boldsymbol{p}$ becomes (Ryder, 1996, p. 402):

$$\boldsymbol{p} \to \boldsymbol{p}' = \boldsymbol{p} - q_{\mathrm{e}}\boldsymbol{A}, \tag{2.18}$$

or equivalently, the phase ϕ_Ψ changes by

$$\phi_\Psi \to \phi'_\Psi = \phi_\Psi - q_{\mathrm{e}}\boldsymbol{A}\cdot\boldsymbol{r}. \tag{2.19}$$

Consider a closed circular path, l, on a sphere centered at the origin with a fixed radius r. Additionally, it is parallel to the xy-plane with a polar angle θ as seen in Fig. 2.1. The total change in phase, $\Delta\phi_\Psi$, can be calculated by integrating with respect to the azimuthal angle ϕ from 0 to 2π:

$$\Delta\phi_\Psi = q_{\mathrm{e}}\oint_l \boldsymbol{A}\cdot d\boldsymbol{l} = q_{\mathrm{e}}\int_S (\nabla\times\boldsymbol{A})\cdot d\boldsymbol{S} = q_{\mathrm{e}}\int_S \boldsymbol{B}\cdot d\boldsymbol{S} = q_{\mathrm{e}}\Phi_{\mathrm{m}}(\theta)\,. \tag{2.20}$$

First off, Stokes's theorem is invoked to change a line integral into a surface one. The relationship between these two integrals is also shown in Fig. 2.1. The first line integral in equation (2.20) was performed on the closed path l, which is also the boundary of the shaded surface S—a smaller spherical cap. Stokes's theorem states that, the line integral of vector field $\boldsymbol{A}$ on l is equivalent to the surface integral of the curl of $\boldsymbol{A}$